Hindawi Publishing Corporation
Journal of Chemistry
Volume 2015, Article ID 276768, 12 pages
http://dx.doi.org/10.1155/2015/276768

Research Article

Photodegradation of Polyphenols and Aromatic Amines in Olive Mill Effluents with Ni Doped C/TiO_2

Delia Teresa Sponza and Rukiye Oztekin

Department of Environmental Engineering, Engineering Faculty, Dokuz Eylül University, Tınaztepe Campus, Buca, 35160 İzmir, Turkey

Correspondence should be addressed to Delia Teresa Sponza; delya.sponza@deu.edu.tr

Received 24 October 2014; Accepted 13 January 2015

Academic Editor: Ronaldo F. do Nascimento

Magnetic nickel coated carbon based titanium dioxide [C/TiO_2/Ni] nanocomposites were used for photodegradation of polyphenols and total aromatic amines (TAAs) metabolites from olive mill wastewaters (OMW) at different operational conditions such as different mass ratios of C, TiO_2, and Ni (1%/2%/5%; 5%/1%/2%; and 2%/5%/1%), being at increasing photodegradation times (15, 30, 45, 60, 75, 120, and 180 min), photocatalyst concentrations (100, 250, 500, and 1000 mg L^{-1}), pH values (3.5, 4.0, 7.0, and 10.0) and temperatures (15°C, 25°C, 50°C, and 80°C), and being under 300 W ultraviolet (UV) and 30 W sunlight irradiation. Under the optimized conditions, at pH = 7.0, at 500 mg L^{-1} C/TiO_2/Ni nanocomposite, under 300 W UV light, after 60 min, at 25°C, the maximum $COD_{dissolved}$, total phenol, and TAAs removals were 99%, 90%, and 96%, respectively. Photodegradation removals in the OMW under sunlight and being lower than those under UV light.

1. Introduction

Photocatalysis has been recognized as a potential technique for degradation process, which is being widely applied as one of the most effective methods for wastewater treatment [1]. For instance, it is widely applied as a useful technique for destruction of organic pollutants [2, 3]. TiO_2 semiconductor in anatase form is often used as photocatalyst for water purification from pollutants because of its stability, nontoxicity, and relatively satisfied activity [2, 3]. The high surface area-to-volume ratio of TiO_2 nanoparticles, however, results in their aggregation [2, 3]. To improve the photocatalytic activity of traditional TiO_2, there are a variety of novel visible-light-responsive photocatalysts developed and those photocatalysts showed better catalytic activity [2, 3]. Meanwhile, doped TiO_2 photocatalysts [4, 5] and composite photocatalysts [6–8] were taken into consideration for the treatment of some dyes and pollutants [9]. TiO_2-C hybrids are some of the most extensively investigated and most promising materials to improve the photocatalytic performance of TiO_2 because a variety of carbon materials can be tailor-made to meet the demands of TiO_2 as a photocatalyst [10]. In addition, the lightweight, nonpolar, nonreactive, and nontoxic nature of carbon materials and the easy separation of the materials from water are attractive in wastewater treatment [10]. In recent years, there has been growing interest in hybridizing carbon nanostructures such as carbon nanotubes (C) [8] and graphene [9, 10] with TiO_2 to enhance the photocatalytic performance. The main purpose of carbon materials in the nanocomposite is to transfer photogenerated electrons from TiO_2 to suppress the recombination for effective charge separation [9]. Zhang [11] found that TiO_2/Ni composites have the functions of both TiO_2 and Ni [11]. The photocatalytic and biocompatibility studies show that this TiO_2/Ni composite remains the outstanding photocatalytic activity for organic pollutant decomposition and the biocompatibility of TiO_2 [11]. Lin et al. [12] investigated the hydrogenation of nitrobenzene in water by using Ni/TiO_2 catalyst. This catalyst has been used as an effective photocatalyst for decomposition of organic pollutants [11]. Pirkarami et al. [13] found 70% Reactive Red 19, 75% Acid Orange 7, and 74% Acid Red 18 removals with 30 mg L^{-1} Nano-Ni-TiO_2 photocatalyst at pH = 7.0 and 25°C. Shao et al. [10] studied the photocatalytic degradation of methylene blue (MB) dye with the addition

of photocatalyst carbon-based anatase-type TiO_2 (TiO_2-C) hybrid aerogel nanocomposites. The photocatalytic degradation removal at darkness condition was found as 33% for MB removal while the MB photodegradation removal was found as 98%, at 500 W UV light, after 150 min at TiO_2/C mass ratio of 0.902, at 25°C. The Ni/TiO_2 photocatalysts with a content of Ni about 1.5 mol% photodegraded 0.025 g L^{-1} of methyl orange with a removal efficiency of 87% [14]. On the other hand, C/Ni/TiO_2 nanocomposite is a new class of photocatalyst in CO_2 photoreduction under visible light irradiation [15]. Gondal et al. [9] found 81% removal efficiency for methyl orange by using 0.5 g L^{-1} C_{10}%/TiO_2/Ni under 6 W UV light (λ = 464 nm), at 0.4 g L^{-1} initial Ni concentration, and a C/TiO_2 ratio of 0.08 ratio, after 120 min, at 27°C, respectively. This nanocomposite is suitable for photodegradation of polyphenols and TAAs metabolites in the OMW. The photogenerated electron and hole may recombine if there are no suitable active/reaction sites available on the surface of the light-harvesting semiconductor [9].

Wastewater arising from olive processing is one of the strongest industrial effluents, with chemical oxygen demand (COD) values of up to 220 g L^{-1} and corresponding biochemical oxygen demand (BOD) values of up to 100 g L^{-1}. Besides its strong organic content (BOD_5 35–110 g L^{-1}, COD 45–170 g L^{-1}, suspended solids (SS) 1–9 g L^{-1}), olive mill wastewater (OMW) contains high concentrations of recalcitrant compounds such as lignins and tannins, which give it a characteristic dark color (52 270–180 000 mg L^{-1} Pt-Co units), but, most importantly, it contains phenolic compounds and long-chain fatty acids which are toxic to microorganisms and plants. The concentration of phenolic compounds in OMW varies greatly from 0.5 to 24 g L^{-1}. The high recalcitrant organic load and the associated toxicity require the treatment of OMW. In recent years, there has been growing interest in oxidation and advanced oxidation processes for the treatment of olive mill wastewater. Ozone is a powerful oxidising agent which attacks the compounds containing aromatic rings and double bonds and breaks them down. Small COD reductions of 18–20% were observed after 2 h of ozonation of OMW with an initial COD of 10 g L^{-1}. A number of physical, chemical, and biological treatment methods have been reported in literature, including flotation and sedimentation [16], sand filtration [17, 18], ozonation [19], membrane filtration [20–22], neutralization with addition of acid, advanced chemical oxidation (Fenton reaction) [23, 24], adsorption by activated carbon, and aerobic and anaerobic digestions [25–27] for the removal of the OWW. These methods, however, are limited because they are too expensive to find a wide application and ineffective in meeting stringent effluent standards and could result in huge amount of sludge. The utilization of photocatalysis approach with different nanoparticles for OMW treatment has been successfully reported [28, 29]. However, to the best of our knowledge, there have been no reports on the application of C/Ni/TiO_2 nanocomposites photodegradation technology on the removal of contaminants from the OMW wastewater.

The aim of this study was the synthesis of PAC on Ni/TiO_2 as a new class of photocatalyst for the removal pollutants in the OMW (COD components, polyphenols, and TAAs metabolites). The effects of mass ratios of C/TiO_2/Ni (1%/2%/5%; 5%/1%/2%; and 2%/5%/1%), the effects of increasing concentrations of C/TiO_2/Ni nanocomposites (100, 250, 500, and 1000 mg L^{-1}), increasing photoretention times (15, 30, 45, 60, 75, 120, and 180 min), increasing pH values (3.5, 4.0, 7.0, and 10.0), and increasing temperatures (15, 25, 50, and 80°C) on the pollutant parameters of OMW were studied at 300 W UV light and at 30 W sunlight irradiations.

2. Material and Methods

2.1. Raw Wastewater. The characterization of raw OMW taken from the influent of olive oil production industry in İzmir, Turkey, is given in Table 1. This plant is operated with a three-phase olive oil extraction process.

2.2. Preparation of C/TiO_2/Ni Photocatalyst. Masses of 3.5 g of TiO_2, 3.980 g of $Ni(Ac)_2$, and 2 g of activated carbon were weighed, where the mass ratios of PAC and TiO_2 are 1%, 2%, and 5%, respectively. These three mixed raw materials with the designed proportion were grounded with an agate mortar for 30 min and then sintered in a crucible under N_2(g) atmosphere at 400°C for 2 h, with the temperature rise rate of 20°C min^{-1}. These samples were obtained after annealing and cooling down to the room temperature. The as-prepared composite was named according to the preparation conditions as illustrated by "C/TiO_2/Ni", indicating that "C", "TiO_2" are the raw materials of PAC and TiO_2 powders with anatase phase. The mass ratios of PAC/TiO_2/Ni were adjusted as 1%/2%/5%; 5%/1%/2%; and 2%/5%/1%, respectively.

2.3. X-Ray Diffraction Analysis. XRD patterns of the samples were carried out using a D/Max-2400 Rigaku X-ray powder diffractometer operated in the reflection mode with Cu Ka (λ = 0.15418 nm) radiation through scan angle (2θ) from 10° to 80°.

2.4. Scanning Electron Microscopy (SEM) Analysis. The morphological structures of the C/TiO_2/Ni nanocomposites before photocatalytic degradation with UV and sunlight irradiations and after photocatalytic degradation with UV and sunlight irradiations were observed by means of a SEM.

2.5. Photocatalytic Degradation Reactor. A 2 L cylinder quartz glass reactor was used for the photodegradation experiments in the OMW under 300 W UV and 30 W sunlight irradiations, at different operational conditions. 1000 mL OMW was filled for experimental studies and the photocatalyst was added to the cylinder glass reactor. The reactor was exposed to the sunlight between hours 11.00 and 16.00 in a day during July. The sunlight power was measured with a Zeikon luminometer where the light power was around 30 W at the times mentioned above. The photocatalytic reaction was operated with constant stirring during the photocatalytic degradation process under UV and sunlight irradiations. The temperature was controlled with an automatic temperature changing heater inside the photoreactor. The temperature

Table 1: Characterization values of OMW at pH = 4.5 (n = 3, mean values).

Parameters	Values		
	Minimum	Medium	Maximum
pH_0	4	4.4	4.8
DO_0 (mg L^{-1})	0.01	0.06	0.11
ORP (mV)	+122	+128.5	+135
TSS (mg L^{-1})	55.1	57.65	60.2
COD_{total} (mg L^{-1})	99130	112270	125410
COD_{dis} (mg L^{-1})	87200	102275	117350
COD_{inert} (mg L^{-1})	32460	57230	82000
BOD_5 (mg L^{-1})	64500	82030	99560
BOD_5/COD_{dis}	0.3	0.6	0.9
Total N (mg L^{-1})	198	259	320
NH_4-N (mg L^{-1})	25.2	32.2	39.1
NO_3-N (mg L^{-1})	42	55	68
NO_2-N (mg L^{-1})	19.3	24.2	29.1
Total P (mg L^{-1})	496	638.7	781.4
PO_4-P (mg L^{-1})	352	456.1	560.1
Phenol metabolites (mg L^{-1})			
Catechol	3	16	29
4-Methyl catechol	7	19	31
2-PHE	2	5	8
3-PHE	2	9	16
TAAs (mg L^{-1})	1240	1905	2570
Individual TAAs (mg L^{-1})			
2,4,6-trimethylaniline	49	120	190
Aniline	42	108	174
o-Toluidine	27	94	161
o-Anisidine	48	92	135
Dimethylalanine	11	51	90
Ethylbenzene	20	71	122
Durene [3,6-bis(dimethylamino)]	34	100	123

was adjusted to the desired level and it was studied at constant temperatures of 15, 25, 50, and 80°C for desired time intervals. The pH of the OMW was adjusted to asidic, notral, and alkaline with 1 N NaOH and 1 N HCl. The schematic configuration of the photocatalytic reactor was illustrated in Figure 1. A volume of 10 mL of the reacting solution was sampled and centrifugated (at 10000 rpm) at different time intervals.

2.6. Experimental Chemicals. Nano-TiO_2, nano-$Ni(Ac)_2$, and PAC were purchased from Merck, (Germany). Helium, He(g) (GC grade, 99.98%), and nitrogen, N_2(g) (GC grade, 99.98%), were purchased from Linde (Germany). Catechol (99%), tyrosol (99%), quercetin (99%), caffeic acid (99%), 4-methyl catechol (99%), 2-phenyl-phenol (2-PHE) (99%), 3-phenyl-phenol (3-PHE) (99%), 2,4,6 trimethylaniline (99%), aniline (99%), o-toluidine (99%), o-anisidine (99%), dimethylaniline (99%), ethylbenzene (99%), and durene [3,6-bis(dimethylamino)] (99%) were purchased from Aldrich (Germany).

2.7. Analytical Methods. The pH values, T (°C), ORP, DO, BOD_5, COD_{total}, $COD_{dissolved}$, total suspended solids (TSS), total-N, NH_3-N, NO_3-N, NO_2-N, total-P, and PO_4-P measurements were monitored following the standard methods 2310, 2320, 2550, 2580, 4500-O, 5210 B, 5220 D, 2540 D, 4500-N, 4500-NH_3, 4500-NO_3, 4500-NO_2, and 4500-P [30]. Inert COD was measured according to glucose comparison method [31]. 2,4,6 trimethylaniline, aniline, o-toluidine, dimethylaniline, ethylbenzene, and durene [3,6-bis(dimethylamino)] were identified as TAAs were identified with a high-pressure liquid chromatography (HPLC) (Agilent-1100) with a C-18 reverse phase HPLC column, (25 cm × 4.6 mm × 5 μm, Ace 5 C-18). o-Anisidine was measured in a HPLC (Agilent-1100) with a UV detector at a mobile phase of 35% acetonitrile/65% H_2O at a flow rate of 1.2 mL min^{-1}. Total phenol, catechol, tyrosol, quercetin, caffeic acid, 4-methyl catechol, 2-PHE, and 3-PHE (HPLC, Agilent-1100) with a Spectra system model SN4000 pump and Asahipak ODP-506D column (150 cm × 6 mm × 5 μm).

Irradiations of 300 W UV light power and 30 W sunlight power were used for the photocatalytic degradation of

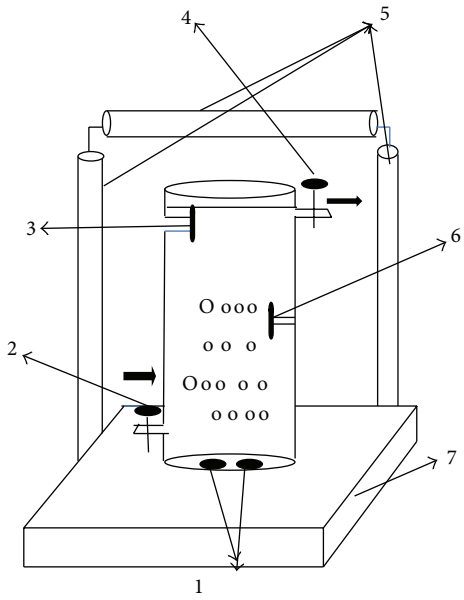

Figure 1: The shematic configuration of the photocatalytic reactor (1) magnets, (2) the inlet of OMW, (3) heater for temperature adjustment, (4) the outlet of OMW, (5) UV or sunlight lamps [each one of UV (100 W ∗ 3) or sunlight (30 W)], (6) pH meter, (7) magnetic stirrer, respectively.

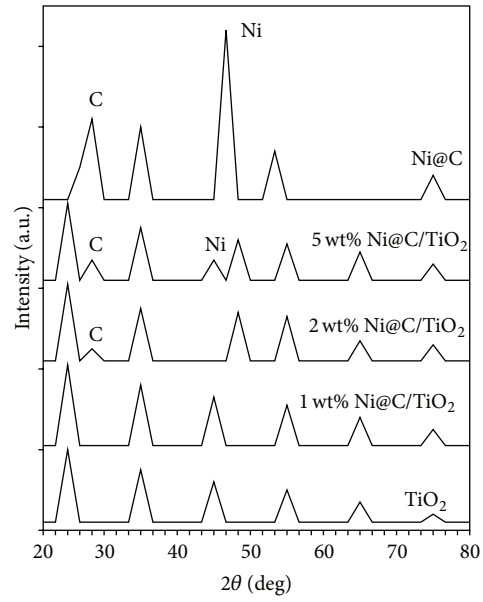

Figure 2: The measured XRD patterns of prepared C/TiO_2/Ni nanocomposites with mass ratios of 1%/2%/5%; 5%/1%/2%, and 2%/5%/1%, respectively.

the pollutant parameters in the OMW, at different pH values (3.5, 4.0, 7.0, and 10.0), different temperatures (15, 25°C, 50°C, and 80°C), different retention times (15, 30, 45, 60, 75, 120, and 180 min), and different C/TiO_2/Ni nanocomposite photocatalyst concentrations (100, 250, 500, and 1000 mg L^{-1}).

All experiments were carried out three times and the results were given as the means of triplicate samplings.

3. Results and Discussion

3.1. XRD Analysis Results. The measured XRD patterns of prepared C/TiO_2/Ni nanocomposites with mass ratios of 1%/2%/5%; 5%/1%/2%; and 2%/5%/1%, respectively, are shown in Figure 2. The main diffraction peaks of various products can be ascribed to anatase TiO_2, while the peaks at 2 h = 26.5 for the graphite-like carbon can also be detected once the C/TiO_2/Ni mass ratio was 1%/2%/5%. The metal Ni species is high when the C/TiO_2/Ni mass ratio was 5%/1%/2%. C species can be seen from the XRD pattern, and the nanocomposites with C/TiO_2/Ni mass ratio of 2%/5%/1%, TiO_2, show the relative diffraction peaks, implying that part of TiO_2 might be oxidized and/or lost during the preparation process.

3.2. SEM Analysis Results. Figure 3(a) is a SEM image of mixture of C/Ni/TiO_2. The microparticles are essentially spherical in shape and have a narrow size distribution of 0.8–1.0 μm before photocatalytic oxidation. Figure 3(b) indicates that the core-shell Ni/TiO_2 composite was coated with polyphenols and aromatic amines.

3.3. FTIR Analysis Results. The FTIR spectra of C-TiO_2 samples are shown in Figure 4. The peaks at about 3400 and 1630 cm^{-1} with similar intensities are associated with the stretching vibrations of water molecules, including hydroxyl groups and molecular water.

3.4. Effect of Mass Ratios of Ni/C/TiO_2 on the OMW Pollutant Parameters. The photocatalytic performance of the synthesized catalyst sample which is combined with three different C/TiO_2/Ni mass ratios of 1%/2%/5%, 5%/1%/2%, and 2%/5%/1%. The maximum photodegradation efficiency was obtained at 2%/5%/1% mass ratio of Ni/C/TiO_2 which is the maximum carbon which can act as photosensitizer, absorbing the UV and sun lights, which can inject the photogenerated electrons into TiO_2 conduction band as mentioned in the study performed by Zeng et al. [15] (Table 2). In other words, the interfacial behavior between C and TiO_2 may increase the photogenerated electron mobility in TiO_2. Meanwhile, the synergetic effect of the intrinsic properties of Ni and component in the present nanocomposite is also beneficial for the electron transfer in the conduction band to reduce the pollutants (COD, total phenols and TAAs) in the OMW. Approximately similar photodegradation removals were obtained for Ni/C/TiO_2 mass ratios of 1%/2%/5% (the removals are very slightly lower than the removal efficiencies at 2%/5%/1% C/TiO_2/Ni mass ratio), since with high TiO_2 mass ratio more electrons were activated by production of high OH radicals resulting in high pollutant photodegradation in the OMW (Table 2). The effect of high Ni mass ratios in the Ni/C/TiO_2 nanocomposite formation (5%/1%/2%) was found to be not so significant. However, higher pollutant photodegradation removals were obtained for this Ni mass ratio (Table 2). The slightly lower photodegradation removals

Table 2: Effect of mass ratios of C/TiO_2/Ni nanocomposites (1%/2%/5%, 5%/1%/2%, and 2%/5%/1%) and increasing retention times on the removals of OMW during photocatalytic degradation, at 500 mg L^{-1} C/TiO_2/Ni nanocomposite, under 300 W UV and 30 W sunlights, at pH = 7.0, and at 25°C (n = 3, mean values).

Retention time (min)	C/TiO_2/Ni	Removal efficiencies (%)							
		UV light Parameters (mg L^{-1})				Sunlight Parameters (mg L^{-1})			
		COD_{total}	COD_{dis}	Total phenol	TAAs	COD_{total}	COD_{dis}	Total phenol	TAAs
15	1%/2%/5%	44	42	38	54	42	39	35	46
	2%/5%/1%	55	53	59	70	54	51	55	68
	5%/1%/2%	50	49	50	52	45	40	44	50
30	1%/2%/5%	49	45	40	56	46	41	37	48
	2%/5%/1%	57	56	61	72	56	54	59	70
	5%/1%/2%	51	50	52	58	47	44	46	55
45	1%/2%/5%	53	51	47	67	50	49	43	64
	2%/5%/1%	72	70	67	88	70	67	64	87
	5%/1%/2%	56	55	58	64	51	53	50	61
60	1%/2%/5%	88	86	82	80	85	83	79	77
	2%/5%/1%	99	99	90	96	96	95	88	91
	5%/1%/2%	90	85	78	82	86	81	75	79
75	1%/2%/5%	86	85	77	78	83	81	74	75
	2%/5%/1%	97	95	86	95	94	93	80	90
	5%/1%/2%	84	81	73	79	81	76	71	74
120	1%/2%/5%	85	82	71	75	82	78	68	70
	2%/5%/1%	94	93	79	92	92	91	75	89
	5%/1%/2%	76	73	66	74	73	67	62	71
180	1%/2%/5%	81	80	67	72	80	75	64	69
	2%/5%/1%	90	89	76	90	89	87	68	88
	5%/1%/2%	74	72	64	71	68	63	59	67

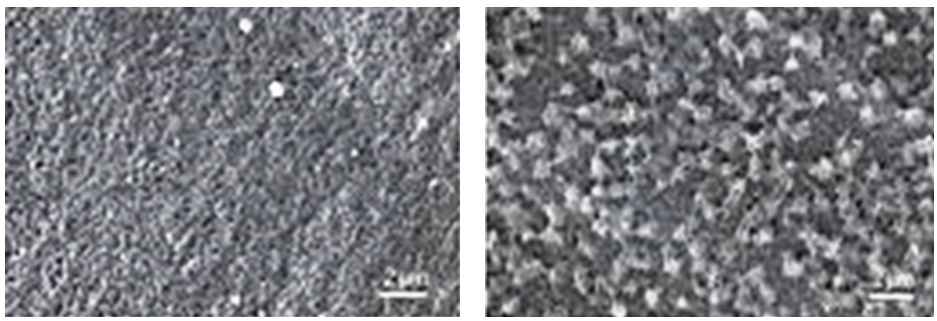

(a) (b)

Figure 3: The SEM images of (a) a mixture of C/Ni/TiO_2 before photocatalytic oxidation and (b) the core-shell Ni/TiO_2 composite coated with polyphenols and aromatic amines.

can be discussed as follows. The weakly bounded Ni on the stoichiometric TiO_2 surface tends to migrate and aggregate to form larger clusters on TiO_2 [32]. The electron localization and a different surface chemistry take place during the removal of neutral oxygen from the TiO_2 surface and charge transfer between Ni clusters and TiO_2 substrate takes place at the interfaces. The substrate surface treatment influences the oxidation state of Ni. The chemical environment change upon Ni deposition and the defect structures on NiO surfaces have been assigned to the Ni^{+3} species existing on the surface [32]. Generally, modification of TiO_2 by Ni did not enhance the photooxidation of pollutants and obtained results were slightly lower than those obtained using TiO_2. The modification of the surface by Ni is connected with the affordability of TiO_2 and the excess of Ni compared to Ti may inhibit the photooxidation (the removals were very slightly lower than the removal efficiencies at 1%/2%/5% C/TiO_2/Ni mass ratio).

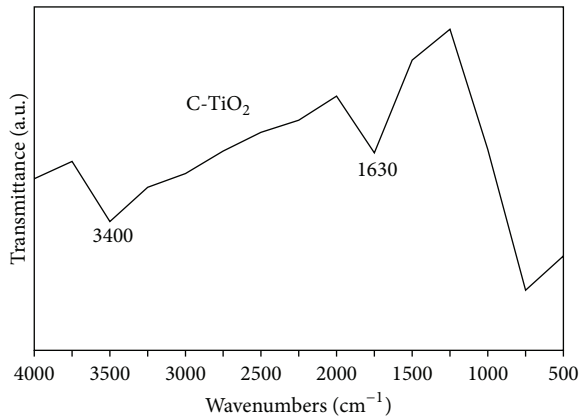

Figure 4: The FTIR spectra of C-TiO_2 samples.

3.5. Establishment of the Optimum Retention Time for Photocatalytic Degradation of the Pollutants in the OMW. The effects of increasing retention times (15, 30, 45, 60, 75, 120, and 180 min) on the photocatalytic degradation of pollutant parameters in the OMW, under 300 W UV and 30 W sunlight, at 500 mg L^{-1} C/TiO_2/Ni nanocomposites, at pH = 7.0, at room temperature (25°C) are shown in Table 2. The maximum COD_{total}, COD_{dis}, total phenols, and TAAs removals in the OMW were 99%, 99%, 90%, and 96%, respectively, under 300 W UV light, at 500 mg L^{-1} C/TiO_2/Ni nanocomposites, at pH = 7.0, at 25°C, after 60 min, respectively (Table 2). The maximum COD_{total}, COD_{dis}, total phenols, and TAAs removals in the OMW were 96%, 95%, 88%, and 91%, respectively, under 30 W sunlight, at 500 mg L^{-1} C/TiO_2/Ni nanocomposites, at pH = 7.0, at 25°C, after 60 min, respectively (Table 2). As the photodegradation times were increased from 15 min up to 60 min in the presence of 500 mg L^{-1} C/TiO_2/Ni nanocomposite, photodegradation removals were increased in all pollutant parameters in the OMW under 300 W UV light (Table 2). Similarly, the removal efficiencies increased as the contact time between pollutants and 500 mg L^{-1} C/TiO_2/Ni nanocomposite increased from 15 min to 60 min in the OMW, under 30 W sunlight. On the other hand, the removals of pollutant parameters in the OMW decreased in the same UV and sunlight as the increasing retention times from 75 to 180 min, respectively (Table 2). Low contact times cannot be enough for OH radical production throughout photooxidation process while high contact times could have decomposed the structure and the pores of C/TiO_2/Ni nanocomposite, and the photocatalysts might have been covered completely with the particles of pollutants. Therefore, the maximum removal efficiencies were observed at 60 min retention time during the experimental studies (Table 2).

3.6. Effect of Different C/TiO_2/Ni Nanocomposite Concentrations on the Photocatalytic Degradation of the Pollutants in the OMW. Since the maximum photodegradation removals of C/TiO_2/Ni nanocomposite were obtained with mass ratio of 2%/5%/1%, the studies were performed with this form of the nanocomposite synthesized under laboratory conditions. The rate of photocatalytic reaction and the removal of pollutants in the OMW are strongly influenced by the amount of the photocatalyst. Heterogeneous photocatalytic reactions are known to show proportional increase in photodegradation with catalyst loading. Generally, in any given photocatalytic application, the optimum catalyst concentration must be determined in order to avoid excess usage of catalyst and to ensure the total absorption of efficient photons. As shown in Table 3, four different C/TiO_2/Ni nanocomposite concentrations (100, 250, 500, and 1000 mg L^{-1}) were used to determine the maximum removals of pollutant parameters (COD components (COD_{total}, COD_{dis}, and COD_{inert}), polyphenols (catechol, tyrosol, quercetin, caffeic acid, 4-methyl catechol, 2-PHE, and 3-PHE), and TAAs metabolites (2,4,6 trimethylaniline, aniline, o-toluidine, o-anisidine, dimethylaniline, ethylbenzene, and durene), resp.) in the OMW throughout photocatalytic degradation, under UV and sunlight. The maximum COD_{total}, COD_{dis}, and COD_{inert} removals in the OMW were 99%, 99%, and 73%, respectively, under 300 W UV light, at 500 mg L^{-1} C/TiO_2/Ni nanocomposite, at pH = 7.0, at 25°C, after 60 min, respectively (Table 3). The maximum removals of total phenols and polyphenols were between 86 and 90%, under 300 W UV light, at 500 mg L^{-1} C/TiO_2/Ni nanocomposites, at pH = 7.0, at 25°C, after 60 min, respectively (Table 3). The maximum removal efficiencies of TAAs and TAAs metabolites, such as 2,4,6 trimethylaniline, aniline, o-toluidine, o-anisidine, dimethylaniline, ethylbenzene, and durene, in the OMW were between 80 and 96%, under 300 W UV light, at 500 mg L^{-1} C/TiO_2/Ni nanocomposites, at pH = 7.0, at 25°C, after 60 min, respectively (Table 3). On the other hand, the removal efficiencies of pollutant parameters (COD components, polyphenols, and TAAs metabolites) increased as the C/TiO_2/Ni nanocomposites concentrations were increased from 100 to 250 mg L^{-1} under 300 W UV light. Therefore, the removal efficiencies of the pollutant parameters (COD components, polyphenols, and TAAs metabolites) were slightly decreased from 500 to 1000 mg L^{-1} C/TiO_2/Ni nanocomposites concentrations under 300 W UV light (Table 3). The observation was that removal efficiency increased as the quantity of the nanocomposite was increased. However, in this study low photodegradation removals were observed with low (100 mg L^{-1}) and high (1000 mg L^{-1}) C/TiO_2/Ni concentrations. The inhibition effect of over loaded photocatalysts concentrations for the pollutant parameter removals in the OMW was detected. Probably the structural decomposition of photocatalysts and the pore surfaces of photocatalysts might have been covered completely with the particles of pollutant parameters (COD_{total}, COD_{dis}, total phenols, and TAAs) or other radical species (carbon based radicals, e.g., $CO_3^{\bullet}$ radicals, etc.). The effect of photocatalyst quantity can be explained by the fact that decreasing the amount of photocatalyst decreases the number of active sites on the Ni-TiO_2 surface, which in turn decreases the numbers of hydroxyl ($OH^{\bullet}$) and hydroperoxyl ($OH_2^{\bullet}$) radicals.

The maximum COD_{total}, COD_{dis}, and COD_{inert} removals in the OMW were 96%, 95%, and 70%, respectively, under 30 W sunlight, at 500 mg L^{-1} C/TiO_2/Ni nanocomposites, at

Table 3: Effect of increasing $C/TiO_2/Ni$ nanocomposite concentrations on the removals of OMW during photocatalytic degradation, under 300 W UV and 30 W sunlight irradiations, at pH = 7.0, and at 25°C, after 60 min ($n = 3$, mean values).

Parameters (mg L^{-1})	Removal efficiencies (%)							
	UV light				Sunlight			
	$C/TiO_2/Ni$ nanocomposites (mg L^{-1})				$C/TiO_2/Ni$ nanocomposites (mg L^{-1})			
	100	250	500	1000	100	250	500	1000
COD_{total}	57	72	99	94	56	70	96	92
$COD_{dissolved}$	56	70	99	93	54	67	95	91
COD_{inert}	39	48	73	65	37	46	70	61
Total phenol	61	67	90	89	59	64	88	85
Polyphenols								
Catechol	59	66	87	85	57	63	84	82
Tyrosol	58	64	89	86	55	59	87	80
Quercetin	54	67	90	89	52	64	88	79
Caffeic acid	56	63	88	81	55	61	86	76
4-Methyl catechol	50	64	89	83	48	62	85	80
2-PHE	57	65	88	86	54	63	82	82
3-PHE	59	67	86	84	56	62	83	81
TAAs	72	88	96	92	70	87	91	90
TAAs Metabolites								
2,4,6 trimethlyaniline	53	64	88	84	51	61	85	81
Aniline	58	63	86	82	57	60	83	79
o-Toluidine	59	67	85	81	58	65	81	77
o-Anisidine	48	65	93	89	46	63	90	86
Dimethylaniline	49	65	95	92	47	60	92	89
Ethylbenzene	56	67	94	90	55	64	91	88
Durene [3,6-bis(dimethylamino)]	50	62	80	78	48	59	78	75

pH = 7.0, at 25°C, after 60 min, respectively (Table 3). The maximum removal efficiencies of total phenols and polyphenols were between 82 and 88% under 30 W sunlight, at 500 mg L^{-1} $C/TiO_2/Ni$ nanocomposites, at pH = 7.0, at 25°C, after 60 min, respectively (Table 3). The maximum removals of all pollutant parameters in the OMW were between 78 and 92%, under 30 W sunlight, at 500 mg L^{-1} $C/TiO_2/Ni$ nanocomposites, at pH = 7.0, at 25°C, after 60 min (Table 3). The result of the photocatalytic degradation removals of the pollutant parameters in the OMW with $C/TiO_2/Ni$ under sunlight showed that the removals were slightly lower than the photocatalytic degradation removals of the pollutant parameters in the OMW under UV light. In addition, the pollutant parameters (COD components, polyphenols, and TAAs metabolites) removal efficiencies were increased from 100 to 250 mg L^{-1} $C/TiO_2/Ni$ nanocomposites concentrations under 30 W sunlight. However, the removal efficiencies of the pollutant parameters (COD components, polyphenols, and TAAs metabolites) were slightly decreased from 500 to 1000 mg L^{-1} $C/TiO_2/Ni$ nanocomposite concentrations under 30 W sunlight (Table 3). A removal of 87% of total polyphenols, compared to 58% removal of COD, was determined after 24 h exposure to 365 nm UV light (at 7.6 W m^{-2}), at 25°C, at pH = 8.0 [33]. In this study, the 99% COD_{dis} and 90% total phenol removals (Table 3) are higher than the removals observed by Baransi et al. [33] as mentioned above.

3.7. Establishment of Optimum Temperature Value for Photocatalytic Degradation of the OMW Pollutants with $C/TiO_2/Ni$. The effect of increasing temperature values (15, 25, 50, and 80°C) on the photocatalytic degradation of the OMW pollutants was investigated, under 300 W UV and 30 W sunlight, at optimum photocatalyst concentration (500 mg L^{-1} $C/TiO_2/Ni$ nanocomposite), at optimum pH value (pH = 7.0), at optimum retention time (60 min). The increasing of temperature values from 15 to 25°C showed a raise in the removal efficiencies of OMW pollutants in both UV conditions. The maximum COD_{total}, COD_{dis}, total phenols, and TAAs removals in the OMW were 99%, 99%, 90%, and 96%, respectively, under 300 W UV light, at pH = 7.0, at 25°C, after 60 min, respectively (Table 4). The removal efficiencies of COD_{total}, COD_{dis}, total phenols, and TAAs in the OMW were 96%, 95%, 88%, and 91%, respectively, under 30 W sunlight, at 500 mg L^{-1} $C/TiO_2/Ni$ nanocomposite, at pH = 7.0, at 25°C, after 60 min, respectively (Table 4). The photodegradation removals of the pollutant parameters decreased as the temperature increased from 25 to 50 and to 80°C in both types of irradiation light (Table 4). Therefore,

Table 4: Effect of increasing temperature values on the removals of OMW during photocatalytic degradation, at 500 mg L^{-1} C/TiO_2/Ni nanocomposites, under 300 W UV and 30 W sunlight irradiations, after 60 min, at pH = 7.0. (n = 3, mean values).

Parameters (mg L^{-1})	Removal efficiencies (%)							
	UV light T (°C)				Sunlight T (°C)			
	15	25	50	80	15	25	50	80
COD_{total}	81	99	96	72	79	96	93	71
$COD_{dissolved}$	79	99	95	71	76	95	92	68
COD_{inert}	70	73	68	55	67	70	66	52
Total phenol	85	90	86	69	82	88	82	65
Polyphenols								
Catechol	80	87	85	63	76	84	82	60
Tyrosol	82	89	77	65	77	87	71	57
Quercetin	84	90	85	64	80	88	81	61
Caffeic acid	79	88	86	67	78	86	79	64
4-Methyl catechol	82	89	79	57	75	85	74	55
2-PHE	80	88	86	68	79	82	80	64
3-PHE	78	86	84	69	76	83	82	63
TAAs	89	96	91	73	85	91	87	67
TAAs metabolites								
2,4,6 trimethlyaniline	80	88	86	71	76	85	84	65
Aniline	76	86	85	70	74	83	82	66
o-Toluidine	75	85	84	68	73	81	83	64
o-Anisidine	82	93	91	65	78	90	86	63
Dimethylaniline	84	95	90	67	80	92	87	66
Ethylbenzene	80	94	91	68	77	91	85	62
Durene [3,6-bis(dimethylamino)]	72	80	76	70	69	78	73	66

the optimum operational temperature was selected as 25°C (room temperature) for the maximum removals of pollutant parameters in OMW during photocatalytic degradation.

Numerous studies have been conducted to detect the dependence of photocatalytic reaction on the reaction temperature [34, 35]. Although most of the previous investigations stated that an increase in photocatalytic reaction temperature promotes the recombination of charge carriers and disfavours the adsorption of organic compounds onto the TiO_2 surface [36], at 25°C, more carbon enters into the Ni/TiO_2 composite and the doped carbon content increases, probably, consequently, the absorbance of visible light increases significantly and the band gap energy reduces. When increasing the treating temperature to 50 and 80°C, the doped carbon was released, resulting in the decreased visible light absorbance. Generally, the photocatalytic activity is proportional to low and high light intensities. At low and high temperatures the visible light absorbance could contribute to the decrease of the photocatalytic activity. Therefore, the enhanced visible light activity at 25°C in C-doped Ni/TiO_2 can be partly explained by the broadened light absorbance.

3.8. Establishment of the Optimum pH Value for Photocatalytic Degradation in the OMW. Table 5 shows the effect of increasing pH values (3.5, 4.0, 7.0, and 10.0) throughout photocatalytic degradation on the removals of OMW, under 300 W UV and 30 W sunlight, at optimum retention time (60 min), at room temperature (25°C), at optimum photocatalyst concentration (500 mg L^{-1} C/TiO_2/Ni nanocomposites). The maximum COD_{total}, COD_{dis}, total phenols, and TAAs removals in the OMW were 99%, 99%, 90%, and 96%, respectively, under 300 W UV and 30 W sunlight, at 500 mg L^{-1} C/TiO_2/Ni nanocomposites, at pH = 7.0, at 25°C, after 60 min, respectively (Table 5). The photodegradation removal efficiencies decreased as the pH was decreased from 7.0 to 3.5, under both UV and sun lights, at 500 mg L^{-1} C/TiO_2/Ni nanocomposites, at 25°C, after 60 min, respectively (Table 5). Similarly, the photodegradation removal efficiencies decreased as the pH was increased from 7 up to 10 for the same operational conditions (Table 5). This phenomenon may be attributed to the fact that, as pH is neutral, the concentration of OH ions also increases, thus causing Ni-TiO_2 to generate OH^- and O^{2-} more efficiently. However, it is also seen that the rate of removal diminished for the values beyond pH = 7.0. This is possibly because, at higher pH values, the negatively charged photocatalyst surface repulses the pollutant anions, thereby reducing all pollutant efficiencies in the OMW. The lower photodegradation rate of the phenolic and aromatic compounds at pH = 10.0 is likely a result of the low adsorption onto the surfaces of C/TiO_2/Ni nanocomposites. Another explanation regarding the languor of the process at high pH levels is the presence

Table 5: Effect of increasing pH values on the removals of OMW during photocatalytic degradation, at 500 mg L^{-1} C/TiO_2/Ni nanocomposites, under 300 W UV and 30 W sunlight irradiations, after 60 min, at 25°C (n = 3, mean values).

Parameters (mg L^{-1})	Removal efficiencies (%)							
	UV light pH values				Sunlight pH values			
	3.5	4.0	7.0	10.0	3.5	4.0	7.0	10.0
COD_{total}	82	98	99	69	80	95	96	66
$COD_{dissolved}$	80	97	99	66	77	94	95	62
COD_{inert}	69	71	73	56	68	69	70	53
Total phenol	86	88	90	65	83	84	88	60
Polyphenols								
Catechol	81	85	87	58	75	82	84	55
Tyrosol	83	88	89	60	76	84	87	58
Quercetin	85	87	90	59	79	81	88	56
Caffeic acid	80	86	88	62	78	83	86	59
4-Methyl catechol	83	87	89	52	74	81	85	50
2-PHE	81	85	88	63	77	80	82	59
3-PHE	79	84	86	65	80	82	83	58
TAAs	90	93	96	68	86	89	91	62
TAAs metabolites								
2,4,6 trimethlyaniline	80	86	88	66	76	83	85	60
Aniline	78	83	86	65	75	81	83	61
o-Toluidine	76	84	85	62	74	80	81	59
o-Anisidine	83	91	93	49	79	88	90	45
Dimethylaniline	85	93	95	50	81	89	91	48
Ethylbenzene	82	90	94	60	78	89	91	57
Durene [3,6-bis(dimethylamino)]	73	78	80	64	70	74	78	62

of carbonate (CO_3^{2-}) ions, which could scavenge the $OH^{\bullet}$, or holes produced on the activated TiO_2 surface, comprising a less reactive carbonate ($CO_3^{\bullet}$) radical, slowing the degradation and mineralization process. Samples prepared at neutral pH exhibit more surface area and higher reactivity than those prepared at lower and higher pH. Photocatalytic degradation process for optimum operational conditions was explained.

3.9. Photodegradation Mechanisms of Magnetic C/TiO_2/Ni Nanocomposites. Overall, the mechanism of photocatalysis can be divided into five steps: (1) transfer of reactants in the fluid phase to the surface; (2) adsorption of the reactants; (3) reaction in the adsorbed phase; (4) desorption of the products; and (5) removal of products from the interface region [37]. A photocatalyst is a substance that, after being irradiated by light, can induce a chemical reaction in such a way that the actual substance of the catalyst will not be consumed [38]. It is well known that the photocatalytic activity could be controlled by varieties of factors such as surface area, phase structure, interfacial charge transfer, and separation efficiency of photoinduced electrons and holes. In this work, PAC molecule, acting as an electron shuttle, was mostly in contact with the surface of TiO_2/Ni composite so that it could effectively transfer the photoelectrons from conduction band of TiO_2/Ni composite after being illuminated under UV light irradiation. Therefore, the photogenerated electrons in the magnetic C/TiO_2/Ni photocatalyst could easily migrate from the inner region to the surface to take part in the surface reaction. A new magnetic TiO_2-based photocatalyst combined with PAC and Ni is that which was prepared through a facile pyrolysis reaction [9]. Such series magnetic photocatalysts can be easily recycled from the aqueous solution because of the soft magnetism feature of combined Ni particles. The photocatalytic performance and the enhanced photocatalytic mechanism occurred on the interface of C-TiO_2 [9]. The storing and shuttling photoinduced electrons role of PAC in a photocatalytic process is realized by contacting the surface of TiO_2 with the nanoparticles of PAC. It is the electronic contact between TiO_2 and PAC that leads to the efficient separation of electron-hole pairs to reduce electron-hole recombination, which performs high photocatalytic activity under UV light irradiation [39–41]. The mechanism of photodegradation of polyphenols, COD, and TAAs on C/TiO_2/Ni nanocomposite surface was as follows. The excitation of C/TiO_2/Ni nanocomposite by solar energy leads to the formation of an electron-hole pair. The

hole combines with water (H_2O) to form hydroxyl radicals ($OH^\bullet$) while electron converts oxygen (O_2) to superoxide radical ($O_2^{\bullet -}$), a strong oxidizing species as shown in the following:

$$\text{magnetic C/TiO}_2\text{/Ni nanocomposite} + h\nu \rightleftharpoons \text{magnetic C/TiO}_2\text{/Ni nanocomposite} + h^+_{VB} + e^-_{CB} \quad (1)$$

$$\text{magnetic C/TiO}_2\text{/Ni nanocomposite} + h\nu \rightleftharpoons \text{magnetic C/TiO}_2\text{/Ni nanocomposite } \left(h^+_{VB} + e^-_{CB}\right) \quad (2)$$

$$\text{magnetic C/TiO}_2\text{/Ni nanocomposite} \mid OH^- + h^+_{VB} \longrightarrow \text{magnetic C/TiO}_2\text{/Ni nanocomposite} \mid OH^\bullet \quad (3)$$

$$\text{magnetic C/TiO}_2\text{/Ni nanocomposite} \mid OH_2 + h^+_{VB} \longrightarrow \text{magnetic C/TiO}_2\text{/Ni nanocomposite} \mid OH^\bullet + H^+ \quad (4)$$

$$\text{magnetic C/TiO}_2\text{/Ni nanocomposite} \mid OH^\bullet + \text{Red}_{org} \longrightarrow Ox_{org} \longrightarrow \text{photodegradation of OMW pollutants} \quad (5)$$

$$h^+_{VB} + \text{Red}_{org} \longrightarrow Ox_{org} \longrightarrow \text{photodegradation of OMW pollutants} \quad (6)$$

$$OH^\bullet + OH^\bullet \longrightarrow H_2O_2 \quad (7)$$

$$H_2O_2 \left(\text{or } 2OH^\bullet\right) \longrightarrow 2H^+ + O_2 \quad (8)$$

COD, polyphenols, and TAAs are degraded via photooxidation process by reacting with both $OH^\bullet$ radicals and h^+_{VB} (according to equations (1) → (2), (3) → (4), and (1) → (5)). The $OH^\bullet$ shows electrophilic character and prefers to attack electron rich ortho- or paracarbon atoms of COD, polyphenols, and TAAs. This results in the formation of polyphenol metabolites (catechol, tyrosol, quercetin, caffeic acid, 4-methyl catechol, 2-PHE, and 3-PHE) from total phenol and TAAs metabolites {2,4,6-trimethylaniline, aniline, o-toluidine, o-anisidine, dimethylalanine, ethylbenzene, and durene [3,6-bis(dimethylamino)]} from TAAs are formed with photodegradation process in the OMW under UV and sunlight irradiations, respectively. Radicals undergo further reaction with dissolved oxygen (DO) in the OMW to remove polyphenol metabolites (catechol, tyrosol, quercetin, caffeic acid, and 4-methyl catechol) and TAAs metabolites (2,4,6-trimethylaniline, aniline, o-toluidine, o-anisidine, and dimethylalanine) with simultaneous generation of hydrogen peroxide (H_2O_2) and oxygen radicals ($O_2^\bullet$). The superoxide ($O_2^{\bullet -}$) produces H_2O_2 and O_2 again by disproportion, and generation of $OH^\bullet$ radical accompanied with the production and consumption of H_2O_2.

When the electrons in TiO_2 (anatase phase) are irradiated by UV rays they can be excited from the valence band to the conduction band to generate electron-hole pairs [42]. The holes created in the valence band can react with H_2O molecules to give hydroxide radicals ($OH^\bullet$) and the photogenerated electrons are sufficiently reduced to produce superoxide (O_2^{-2}). The redox potential of the electron-hole pair permits H_2O_2 formation. Depending on the reaction conditions, the holes, $OH^\bullet$, O_2^{-2}, H_2O_2, and O_2, can play important roles in the photocatalytic reaction mechanism. There are several issues that are important in this process. First, exposing the external surface of TiO_2 particles to light is a prerequisite to make such an excitement happen. Second, the light energy ($E = h\nu$) must exceed the band gap (3.20 eV) of the anatase-type TiO_2; therefore lowering the band gap of TiO_2 or using low wavelength light is needed to increase the light utilization efficiency. Third, the oxidizing species cannot migrate for a long distance and stay near the active centers in the TiO_2 particles. Therefore, polluting molecules have to diffuse to the photoexcited active centers. Fourth, the recombination of positive holes with excited electrons before they react to create active species and centers has to be avoided.

Baransi et al. [33] reported that photodegradation of anaerobically treated and diluted (1/10) OMW by the combined TiO_2-PAC sorbent was observed to the normalized concentration of 100 mg L^{-1} caffeic acid which was operated during the three successive runs. In the first run, an instantaneous and high adsorption of caffeic acid was observed both on the mixture of TiO_2/PAC and on the pure 0.45 g L^{-1} PAC (95% caffeic acid removal within 15 min), at pH = 4.1, at 50 mL OMW, at 25°C, at 365 nm UV light (at 7.6 W m^{-2}) irradiation. The instantaneous adsorption of the caffeic acid on 3 g L^{-1} TiO_2 alone was much lower (40% caffeic acid removal within 15 min), but continuous adsorption and photocatalysis processes led to 95% caffeic acid removal after 24 h, at pH = 4.1, at 50 mL OMW, at 25°C, at UV light. Direct photolysis (in the absence of catalyst or adsorbent) resulted in removal of only 17% of initial caffeic acid within 24 h, at pH = 4.1, at 50 mL OMW, at 25°C, at UV light [33]. In this study, 86% caffeic acid removal found under 300 W UV light, after 60 min, at 25°C, at pH = 7.0, is higher than the removal observed by Baransi et al. [33] as mentioned above.

4. Conclusions

In this study, we examined the photodegradation of pollutant parameters (COD components, polyphenols, and TAAs metabolites) in the OMW under UV and sunlight irradiations, with C/TiO_2/Ni nanocomposites, at optimum operational conditions. The maximum removals of pollutant parameters (COD components, polyphenols and TAAs metabolites) in the OMW reached, under 300 W UV and 30 W sunlight, at 500 mg L^{-1} C/TiO_2/Ni nanocomposite concentration, at a mass ratio of 2%/5%/1%, at pH = 7.0, at 25°C, after 60 min. C/TiO_2/Ni nanocomposite is suitable for photodegradation of polyphenols and TAAs metabolites in the OMW. The high removal efficiency obtained with C/TiO_2/Ni

nanoparticule qualifies that this effect may be caused by the synergetic effect on the interface of TiO_2/Ni and PAC that can promote the photoinduced electron mobility in the surface of TiO_2 and the absorption of PAC particles that bring the high concentration of OMW around TiO_2 particles. Providing such a combination could be a step toward the development of sustainable, reliable, and cost-effective technology for the treatment of agroindustrial wastewaters, which demonstrate high innate resistance to biodegradability.

Conflict of Interests

The authors declare that there is no conflict of interests regarding the publication of this paper.

Acknowledgment

This research study was undertaken in the Environmental Microbiology Laboratory at Dokuz Eylül University, Engineering Faculty, Environmental Engineering Department, İzmir, Turkey. The authors would like to thank this body for providing financial support.

References

[1] M. R. Hoffmann, S. T. Martin, W. Choi, and D. W. Bahnemann, "Environmental applications of semiconductor photocatalysis," *Chemical Reviews*, vol. 95, no. 1, pp. 69–96, 1995.

[2] M. A. Gondal, X. F. Chang, and Z. H. Yamani, "UV-light induced photocatalytic decolorization of Rhodamine 6G molecules over BiOCl from aqueous solution," *Chemical Engineering Journal*, vol. 165, no. 1, pp. 250–257, 2010.

[3] Z. Yi, J. Ye, N. Kikugawa et al., "An orthophosphate semiconductor with photooxidation properties under visible-light irradiation," *Nature Materials*, vol. 9, no. 1, pp. 559–564, 2010.

[4] U. G. Akpan and B. H. Hameed, "The advancements in sol-gel method of doped-TiO_2 photocatalysts," *Applied Catalysis A: General*, vol. 375, no. 1, pp. 1–11, 2010.

[5] P. P. Bidaye, D. Khushalani, and J. B. Fernandes, "A simple method for synthesis of S-doped TiO_2 of high photocatalytic activity," *Catalysis Letters*, vol. 134, no. 1-2, pp. 169–174, 2010.

[6] A. I. Kontos, V. Likodimos, T. Stergiopoulos et al., "Self-organized anodic TiO_2 nanotube arrays functionalized by iron oxide nanoparticles," *Chemistry of Materials*, vol. 21, no. 4, pp. 662–672, 2009.

[7] X. Chang, J. Huang, Q. Tan et al., "Photocatalytic degradation of PCP-Na over BiOI nanosheets under simulated sunlight irradiation," *Catalysis Communications*, vol. 10, no. 15, pp. 1957–1961, 2009.

[8] X. Chang, G. Ji, Q. Sui, J. Huang, and G. Yu, "Rapid photocatalytic degradation of PCP-Na over $NaBiO_3$ driven by visible light irradiation," *Journal of Hazardous Materials*, vol. 166, no. 2-3, pp. 728–733, 2009.

[9] M. A. Gondal, C. Li, X. Chang et al., "Facile preparation of magnetic C/TiO_2/Ni composites and their photocatalytic performance for removal of a dye from water under UV light irradiation," *Journal of Environmental Science and Health Part A: Toxic/Hazardous Substances and Environmental Engineering*, vol. 47, no. 4, pp. 570–576, 2012.

[10] X. Shao, W. Lu, R. Zhang, and F. Pan, "Enhanced photocatalytic activity of TiO_2 -C hybrid aerogels for methylene blue degradation," *Scientific Reports*, vol. 3, article 3018, 2013.

[11] D. Zhang, "Chemical synthesis of Ni/TiO_2 nanophotocatalyst for UV/visible light assisted degradation of organic dye in aqueous solution," *Journal of Sol-Gel Science and Technology*, vol. 58, no. 1, pp. 312–318, 2011.

[12] W. Lin, H. Cheng, J. Ming, Y. Yu, and F. Zhao, "Deactivation of Ni/TiO_2 catalyst in the hydrogenation of nitrobenzene in water and improvement in its stability by coating a layer of hydrophobic carbon," *Journal of Catalysis*, vol. 291, no. 1-2, pp. 149–154, 2012.

[13] A. Pirkarami, M. E. Olya, and S. Raeis Farshid, "UV/Ni-TiO_2 nanocatalyst for electrochemical removal of dyes considering operating costs," *Water Resources and Industry*, vol. 5, pp. 9–20, 2014.

[14] N. Xu, Z. Shi, Y. Fan, J. Dong, J. Shi, and M. Z.-C. Hu, "Effects of particle size of TiO_2 on photocatalytic degradation of methylene blue in aqueous suspensions," *Industrial and Engineering Chemistry Research*, vol. 38, no. 2, pp. 373–379, 1999.

[15] P. Zeng, X. Zhang, B. Chai, and T. Peng, "Efficient photocatalytic hydrogen production over Ni@C/TiO_2 nanocomposite under visible light irradiation," *Chemical Physics Letters*, vol. 503, no. 4–6, pp. 262–265, 2011.

[16] M. Achak, N. Ouazzani, A. Yaacoubi, and L. Mandi, "Caractérisation des margines issues d'une huilerie moderne et essais de leur traitement par coagulation-floculation par la chaux et le sulfate d'aluminium," *Revue des Sciences de l'Eau*, vol. 21, no. 1, pp. 53–67, 2008.

[17] M. Achak, L. Mandi, and N. Ouazzani, "Removal of organic pollutants and nutrients from olive mill wastewater by a sand filter," *Journal of Environmental Management*, vol. 90, no. 8, pp. 2771–2779, 2009.

[18] M. Achak, N. Ouazzani, and L. Mandi, "Treatment of modern olive mill effiuent by infiltration-percolation on a sand filter," *Revue des Sciences de l'Eau*, vol. 22, no. 3, pp. 421–433, 2009.

[19] O. Chedeville, M. Debacq, and C. Porte, "Removal of phenolic compounds present in olive mill wastewaters by ozonation," *Desalination*, vol. 249, no. 2, pp. 865–869, 2009.

[20] C. A. Paraskeva, V. G. Papadakis, E. Tsarouchi, D. G. Kanellopoulou, and P. G. Koutsoukos, "Membrane processing for olive mill wastewater fractionation," *Desalination*, vol. 213, no. 1–3, pp. 218–229, 2007.

[21] H. Dhaouadi and B. Marrot, "Olive mill wastewater treatment in a membrane bioreactor: process feasibility and performances," *Chemical Engineering Journal*, vol. 145, no. 2, pp. 225–231, 2008.

[22] E. O. Akdemir and A. Ozer, "Investigation of two ultrafiltration membranes for treatment of olive oil mill wastewater," *Desalination*, vol. 249, no. 2, pp. 660–666, 2009.

[23] Ç. Y. Gomec, E. Erdim, I. Turan, A. F. Aydin, and I. Ozturk, "Advanced oxidation treatment of physico-chemically pretreated olive mill industry effluent," *Journal of Environmental Science and Health Part B*, vol. 42, no. 6, pp. 741–747, 2007.

[24] A. A. Zorpas and C. N. Costa, "Combination of Fenton oxidation and composting for the treatment of the olive solid residue and the olive mile wastewater from the olive oil industry in Cyprus," *Bioresource Technology*, vol. 101, no. 20, pp. 7984–7987, 2010.

[25] N. Azbar, T. Keskin, and E. C. Catalkaya, "Improvement in anaerobic degradation of olive mill effluent (OME) by chemical pretreatment using batch systems," *Biochemical Engineering Journal*, vol. 38, no. 3, pp. 379–383, 2008.

[26] N. Azbar, T. Keskin, and A. Yuruyen, "Enhancement of biogas production from olive mill effluent (OME) by co-digestion," *Biomass and Bioenergy*, vol. 32, no. 12, pp. 1195–1201, 2008.

[27] F. Boubaker and B. C. Ridha, "Modelling of the mesophilic anaerobic co-digestion of olive mill wastewater with olive mill solid waste using anaerobic digestion model No. 1 (ADM1)," *Bioresource Technology*, vol. 99, no. 14, pp. 6565–6577, 2008.

[28] Y. Ruzmanova, M. Stoller, and A. Chianese, "Photocatalytic treatment of olive mill wastewater by magnetic core titanium dioxide nanoparticles," *Chemical Engineering Transactions*, vol. 32, pp. 2269–2274, 2013.

[29] J. M. Ochando-Pulido, G. Hodaifa, M. D. Víctor-Ortega, and A. Martínez-Ferez, "A novel photocatalyst with ferromagnetic core used for the treatment of olive oil mill effluents from two-phase production process," *The Scientific World Journal*, vol. 2013, Article ID 196470, 9 pages, 2013.

[30] A. D. Eaton, L. S. Clesceri, E. W. Rice, A. E. Greenberg, and M. A. H. Franson, *Standard Methods for the Examination of Water and Wastewater*, American Public Health Association (APHA), American Water Works Association (AWWA), Water Environment Federation (WEF), American Public Health Association (APHA), Washington, DC, USA, 21th edition, 2005.

[31] F. Germirli, D. Orhon, and N. Artan, "Assessment of the initial inert soluble COD in industrial wastewaters," *Water Science and Technology*, vol. 23, no. 4–6, pp. 1077–1086, 1991.

[32] H. Pang, Y. Li, L. Guan, Q. Lu, and F. Gao, "TiO_2/Ni nanocomposites: biocompatible and recyclable magnetic photocatalysts," *Catalysis Communications*, vol. 12, no. 7, pp. 611–615, 2011.

[33] K. Baransi, Y. Dubowski, and I. Sabbah, "Synergetic effect between photocatalytic degradation and adsorption processes on the removal of phenolic compounds from olive mill wastewater," *Water Research*, vol. 46, no. 3, pp. 789–798, 2012.

[34] A. G. Rincón and C. Pulgarin, "Photocatalytical inactivation of *E. coli*: effect of (continuous-intermittent) light intensity and of (suspended-fixed) TiO_2 concentration," *Applied Catalysis B: Environmental*, vol. 44, no. 3, pp. 263–284, 2003.

[35] E. Evgenidou, K. Fytianos, and I. Poulios, "Semiconductor-sensitized photodegradation of dichlorvos in water using TiO_2 and ZnO as catalysts," *Applied Catalysis B: Environmental*, vol. 59, no. 1-2, pp. 81–89, 2005.

[36] U. I. Gaya and A. H. Abdullah, "Heterogeneous photocatalytic degradation of organic contaminants over titanium dioxide: a review of fundamentals, progress and problems," *Journal of Photochemistry and Photobiology C: Photochemistry Reviews*, vol. 9, no. 1, pp. 1–12, 2008.

[37] J.-M. Herrmann, C. Duchamp, M. Karkmaz et al., "Environmental green chemistry as defined by photocatalysis," *Journal of Hazardous Materials*, vol. 146, no. 3, pp. 624–629, 2007.

[38] S. Gelover, P. Mondragón, and A. Jiménez, "Titanium dioxide sol-gel deposited over glass and its application as a photocatalyst for water decontamination," *Journal of Photochemistry and Photobiology A: Chemistry*, vol. 165, no. 1–3, pp. 241–246, 2004.

[39] S. Zhu, T. Xu, H. Fu, J. Zhao, and Y. Zhu, "Synergetic effect of Bi_2WO_6 photocatalyst with C_{60} and enhanced photoactivity under visible irradiation," *Environmental Science and Technology*, vol. 41, no. 17, pp. 6234–6239, 2007.

[40] Y. Zhang, Z.-R. Tang, X. Fu, and Y.-J. Xu, "TiO_2-graphene nanocomposites for gas-phase photocatalytic degradation of volatile aromatic pollutant: is TiO_2-graphene truly different from other TiO_2-carbon composite materials?" *ACS Nano*, vol. 4, no. 12, pp. 7303–7314, 2010.

[41] H. Zhang, X. Lv, Y. Li, Y. Wang, and J. Li, "P25-graphene composite as a high performance photocatalyst," *ACS Nano*, vol. 4, no. 1, pp. 380–386, 2010.

[42] O. Carp, C. L. Huisman, and A. Reller, "Photoinduced reactivity of titanium dioxide," *Progress in Solid State Chemistry*, vol. 32, no. 1-2, pp. 33–177, 2004.